LAWRENCE
LIVERMORE
NATIONAL
LABORATORY

LLNL-JRNL-643690

Boussinesq approximation for Rayleigh-Taylor and Richtmyer-Meshkov instabilities

K. O. Mikaelian

September 15, 2013

Physics of Fluids

Disclaimer

Boussinesq approximation for Rayleigh-Taylor and Richtmyer-Meshkov instabilities

Karnig O. Mikaelian
Lawrence Livermore National Laboratory
Livermore, California 94551

Abstract

We apply numerical and analytic techniques to study the Boussinesq approximation in Rayleigh-Taylor and Richtmyer-Meshkov instabilities. In this approximation one sets the Atwood number A equal to zero except in the acceleration or velocity-jump terms. While this approximation is generally applied to low-A systems, we show that it can be applied to high-A systems also in certain regimes and to the "bubble" part of the instability, i.e., the penetration depth of the lighter fluid into the heavier fluid. We extend the Boussinesq approximation and show that it always overestimates the penetration depth but the error is never more than about 41%.

I. INTRODUCTION AND GENERAL RESULTS

An interface between two fluids becomes unstable when placed in a gravitational field or is subjected to an acceleration $\vec{g}$ normal to the interface. Called the Rayleigh-Taylor (RT) instability,[1,2] it occurs when $\vec{g}$ is directed from the low-density (ρ_A) fluid towards the higher-density (ρ_B) fluid. If the interface is subjected to a shock moving in either direction then another instability, called the Richtmyer-Meshkov (RM) instability[3,4] develops. Here the governing parameter is the jump velocity $\Delta\vec{v} = \int \vec{g} dt$, the integral taken over the period when the interface is subjected to the very large but very brief acceleration induced by the shock. As reviewed by several authors,[5-7] these instabilities operate at all scales – astrophysical to sub-millimeter scales. We are particularly interested in Inertial Confinement Fusion (ICF)[8]. The importance of the RT instability was recognized in the original paper on ICF[9] and has gained even more prominence as recent experiments[10] on the National ignition Facility point to RT and RM instabilities as the culprits preventing ignition.

In their simplest form the instabilities appear as single- or multi-scale perturbations at an interface where they grow and lead to intermixing of the fluids. The progression is usually divided into three stages: Linear, nonlinear, and turbulent. In the linear and nonlinear stages a single-scale perturbation of wavenumber k and amplitude $\eta(t)$ grows with time. The linear and nonlinear stages are divided by the conditions $\eta k << 1$ and $\eta k \geq 1$ respectively.[11] In the third, turbulent regime, there is no unique k characterizing the instability – instead, a multi-scale perturbation of magnitude $h(t)$ evolves and grows wider with time.

In addition to g or Δv, the parameter most prominent in RT and RM instabilities is the Atwood number A defined as $A \equiv (\rho_B - \rho_A)/(\rho_B + \rho_A)$. Compressibility in The RM instability can lead to subtle effects whereby a perturbation can grow even when $A = 0$, but these are rare.[12] By far the majority of cases grow when gA or ΔvA does not vanish. In fact, since gravity couples only to mass (or density), we know that g or Δv can appear only as the combination gA or ΔvA. In another context, before the RT or RM instabilities were known, such an observation led Boussinesq[13] to propose what is universally known as the "Boussinesq Approximation" (B.A), where all density gradients are neglected except for gravity (See also Chandrasekhar[14]). This paper is a study of the B.A. in RT and RM instabilities. In particular we try and answer the following questions: What quantities in RT and RM instabilities can be estimated by the B.A., and how good is the B.A. as a function of the Atwood number A?

Previous studies[15-18], dealing exclusively with the RT instability, applied numerical techniques to low-A systems where the B.A. is appropriate. As far as we know no numerical or analytic techniques have been applied to compare Boussinesq with full results, techniques that we use to answer the two questions posed above.

We can obtain general results by combining dimensional analysis with what is already known about RT and RM instabilities. There are 5 variables: η, k, A, g or Δv, and t. We have pointed out[19] that only 3 dimensionless independent quantities can be formed: $\sqrt{gkt}$ or Δvkt, $\eta_0 k$, and A. As argued above, only gA or ΔvA appear in the incompressible Euler equations (we neglect viscosity). It follows that ηk must be expressed as

$$\eta k = F_{RT}(\sqrt{gAkt}; \eta_0 k, A) \qquad (1a)$$

or

$$\eta k = F_{RM}(\Delta v A k t; \eta_0 k, A). \tag{1b}$$

Other possible combinations are η/η_0, often called the "growth factor," obviously given by $(1/\eta_0 k)F$. Similarly, for the independent variables one may choose $\sqrt{gA/\eta_0}t$ or $\Delta v A t/\eta_0$. These forms are useful for expressing h, the turbulent mixing width, because it depends only on 4 variables (there is no "k") and one must write

$$h/h_0 = G_{RT}(\sqrt{gA/h_0}t; A) \tag{2a}$$

or

$$h/h_0 = G_{RM}(\Delta v A t/h_0; A) \tag{2b}$$

where h_0, like η_0, denotes its value at $t = 0$.

By definition, the Boussinesq amplitudes η^B or h^B are obtained by setting the isolated $A = 0$ in the above equations, such as

$$\eta^B = \frac{1}{k}F(\sqrt{gAk}t \text{ or } \Delta v A k t; \eta_0 k, 0) \tag{3}$$

or

$$h^B = h_0 G(\sqrt{gA/h_0}t \text{ or } \Delta v A t/h_0; 0). \tag{4}$$

To evaluate the B.A. we study the "Boussinesq ratio" R^B defined as

$$R^B \equiv \eta^B/\eta \tag{5}$$

or h^B/h in the turbulent regime. For simplicity of notation we forego the subscripts RT or RM as it will be clear from the context.

Several properties of R^B can be immediately deduced: $R^B(A=0)=1$. Since η and η^B are both equal to η_0 at $t = 0$, $R^B(t=0)=1$. Furthermore, in the linear regime, i.e. $\eta k << 1$, $R^B = 1$. This follows from examining the explicit expressions for the linear regime,

$$\eta = \eta_0 \cosh(\sqrt{gAk}t) \tag{6a}$$

or

$$\eta = \eta_0 (1 + \Delta v A k t) \tag{6b}$$

as given in Refs. 1-4. Notice that A appears only in the combination gA or $\Delta v A$ and there are no "extra" A terms that need to be zeroed out to obtain η^B. Therefore $R^B = 1$.

There are actually two amplitudes, "bubble" and "spike." Bubble refers to the penetration of the low-density fluid into the heavier one, and spike is the opposite. In the linear regime $\eta^{bubble} = -\eta^{spike}$ and $R^B = 1$ is true for both bubbles and spikes.

In the nonlinear stage R^B will be different from 1 and is the subject of the next two sections where an analytic or semi-analytic model is used to estimate R^B. However, more can be said about R^B based on what is generally known about RT and RM instabilities without recourse to any model. Obviously, $R^B(A \approx 0) \approx 1$, the traditional low-$A$ application of the B.A. We are interested in high-A, up to $A \approx 1$ where we expect the B.A. to break down.

It is well-known that bubbles and spikes behave similarly at low A, but as A increases the spikes get longer than the bubbles and develop sharp ends, a behavior noted in the very first laboratory experiments[20] by Lewis following Taylor's analysis. It follows that one should not apply the B.A. to spikes at moderate-to-high A, leaving open the question for the bubbles. We illustrate this behavior in Fig. 1 where we compare two RT problems having the same gA but one with $A = 0.05$ and the other with $A = 0.95$, and also two RM problems having the same $\Delta v A$ but one with $A = 0.10$ and the other with $A = 0.75$. We have used the hydrocode CALE[21] to generate these four problems. Clearly, the spikes are quite different between low-A and high-

A, but the bubbles are similar. For this reason we concentrate on nonlinear bubbles in Secs. II and III. The turbulent regime is taken up briefly in Sec. IV, and conclusions are given in Sec. V.

II. ANALYTIC MODEL

We saw above that outside the relatively small domain $A \approx 0$ the B.A. is not a good approximation for spikes but may still be viable for bubbles. A quantitative comparison can be made from Fig. 1: the spikes in Figs. 1(a) and 1(b) are 1.96 cm and 4.05 cm respectively, widely different, while the bubbles are 1.56 cm and 1.22 cm, a mere 22% difference. Note that the larger A has the smaller bubble. Similarly, the spikes in Figs. 1(c) and 1(d) are 0.91 cm and 1.72 cm, very different, while the bubbles are much closer at 0.77 cm and 0.61 cm (these numbers are obtained by placing tracers at the maximum and minimum locations of the initially sinusoidal interface). Note again that the difference is only 21% and that the larger A has the smaller bubble. Of course the opposite is the case for the spikes, implying that while the B.A. underestimates the spike amplitude (rather obvious given what we know about RT and RM instabilities), it overestimates the bubble amplitude but not by much.

We can extend the B.A. by considering it as the lowest-order term in a Taylor expansion around $A = 0$, keeping gA or $\Delta v A$ fixed, and calculating the next or higher-order terms:

$$\eta = \eta^B + C_1 A/k + O(A^2) + ... \qquad (7)$$

valid for small A and for both RT and RM. The sign of this next-order-term, C_1, determines whether η^B underestimates or overestimates the full η. In the rest of this section we use an analytic model to estimate η^B and C_1 for RT and RM instabilities in the nonlinear regime.

A. RT

We shall use an analytic model[19] based on Layzer's approach[22] as adopted by more recent work[23-26]. A semi-analytic model involving ordinary differential equations will be given in Sec. III. Here we consider the fully analytic expression[19,27]

$$\eta = \eta_0 + \frac{1}{k_L}\ln[\cosh(\sqrt{gA_Lk_L}\,t)] \tag{8}$$

where

$$k_L \equiv c(1+c)(1+A)k/2(1+c+cA-A) \tag{9}$$

and

$$A_L \equiv 2A/(1+c+cA-A)\,. \tag{10}$$

The parameter c appearing above takes on the value 2 for "2D" (two-dimensional) perturbations and the value $c=1$ for "3D" (three-dimensional) perturbations. "2D" refers to curtain-like perturbations which start with $\eta(t=0)=\eta_0\cos kx$ where $k=2\pi/\lambda$, λ being the perturbation wavelength. "3D" refers to an axisymmetric configuration which starts $\eta(t=0)=\eta_0 J_0(\beta_1 r/R)$, r being the radial position normal to the axis. Here J_0 is the Bessel function of order 0, and $\beta_1 \approx 3.832$ is the first zero of J_1. In this "tubular flow" geometry one defines $k=\beta_1/R$, R being the radius of the tube. These two geometries were considered by Layzer whose pioneering work[22] forms the basis of most modern analytic treatments of RT and RM instabilities (for a derivation and generalization see Ref. 27).

The full model proposes using the linear results for $\eta<\eta^*$, defined by

$$\eta^* \equiv 1/k(1+c)\,, \tag{11}$$

and use Eq. (8) for $\eta>\eta^*$. We skip the linear regime, discussed in the Introduction, because the B.A. is exact ($R^B=1$) in that regime.

To calculate η^B from Eq. (8) we zero-out all A except in gA. Considering $k_L = k_L(A)$ and $A_L = A_L(A)$, we obtain

$$\eta^B = \eta_0 + \frac{1}{k_L(0)} \ln[\cosh(\sqrt{gA_L(0)k_L(0)}t)]$$

$$= \eta_0 + \frac{2}{ck} \ln[\cosh(\sqrt{cgAk/(1+c)}t)]. \quad (12)$$

As discussed above, η^B can be considered as the zero-order term in a qualified Taylor expansion around $A = 0$ (qualified because we keep gA fixed). To obtain the next-order term C_1 defined in Eq. (7), we expand Eq. (8) and, after some algebra, find

$$C_1 = [(3-c)x \tanh x - 4\ln(\cosh x)]/c(1+c) \quad (13)$$

where $x \equiv \gamma_L(0)t = \sqrt{gA_L(0)k_L(0)}t = \sqrt{cgAk/(1+c)}t$. We show in the Appendix that $C_1 < 0$ for all x.

The Boussinesq ratio calculated from Eqs. (8) and (12) is plotted in Fig. 2 as a function of $\sqrt{gk}t$ for $c = 1$ and 2 and for 3 values of A. We have taken $\eta_0 = \eta^*$. R^B is not sensitive to η_0 – it appears only as an additive constant in this model, a point discussed more in Sec. III. Note that $R^B_{2D} > R^B_{3D}$.

The asymptotic value of R^B is

$$R^B(\sqrt{gk}t \to \infty) = \sqrt{1+A} \quad (14)$$

independent of c. This implies that the B.A. overestimates the full η by no more than $\sqrt{2}-1$ or ~41%.

B. RM

Essentially the same steps can be repeated for the RM case. The starting formula for the full amplitude is[19,27]

$$\eta = \eta_0 + \frac{1}{k_L}\ln(1+\dot{\eta}_0 k_L t) \tag{15}$$

where $\dot{\eta}_0 = \eta_0 k \Delta v A$ is the initial growth rate as calculated by Richtmyer[3]. The "extra" A factors appear only in k_L defined in Eq. (9). Setting those A's equal to 0 we obtain

$$\eta^B = \eta_0 + \frac{2}{ck}\ln(1+c\dot{\eta}_0 kt/2)\,. \tag{16}$$

The Boussinesq ratio R^B calculated from the above two equations is plotted in Fig. 3 as a function of $\Delta v k t$ for $c=1$ and 2 and for $A=0.25$, 0.50, and 0.75. Note that $R^B_{2D} < R^B_{3D}$ in this case.

C_1, the first-order correction to the B.A., can be calculated by the qualified (i.e. $\dot{\eta}_0 = const.$) Taylor expansion of Eq. (15) around $A=0$. We find

$$C_1 = 4[\frac{x}{1+x} - \ln(1+x)]/c(1+c) \tag{17}$$

where $x \equiv \dot{\eta}_0 k_L(0) t = c\dot{\eta}_0 kt/2 = c\eta_0 k^2 \Delta v A t/2$. As in the RT case we show in the Appendix that $C_1 < 0$, meaning $\eta^B > \eta$ hence $R^B > 1$. In other words the B.A. overestimates the RM bubble although, again, not by much.

III. GONCHAROV'S MODEL[26]

Layzer's potential flow model[22] was for one fluid only, i.e. $A=1$. Goncharov extended[26] it to two fluids, i.e., arbitrary A. The basic idea is to use the linear potentials $\phi \sim e^{\pm ky}$ in the

nonlinear Bernoulli equation, supplanted by a term $\phi \sim y$. Such a term was used by Hecht *et al*. and by Goncharov to satisfy the kinematic and dynamic conditions in potential flow[23,26]. One obtains two ordinary differential equations, one for 2D and another for 3D, which can be combined using the variable c:

$$F_1 \frac{\ddot{\eta}}{D} + F_2 \frac{c^2 k^2 \dot{\eta}^2}{8D^2} + 2gA\eta_2 = 0 \tag{18}$$

where

$$F_1 = 2A\eta_2^2 + c^2 Ak\eta_2 / 2(1+c) - c^2 k^2 / 8(1+c), \tag{19a}$$

$$F_2 = 2A\eta_2^2 + (A + cA - 2c - 1)k\eta_2 / (1+c) + ck^2 (3cA/2 + A - c - 1) / 4(1+c)^2, \tag{19b}$$

$$D = \eta_2 - ck / 4(1+c), \tag{19c}$$

and

$$\eta_2(t) = -ck\left\{1 + \left[(1+c)\eta_0 k - 1\right]e^{-k(1+c)(\eta - \eta_0)}\right\} / 4(1+c). \tag{19d}$$

Eq. (18) reduces to the equations in Ref. 24 if we set $A = 1$ and, if we additionally set $\eta_0 = 0$, to Layzer's equations[22]. The derivation in the above form can be found in Ref. 27.

In general Eq. (18) must be solved numerically. But when $\eta_0 = \eta^*$ it can be solved analytically. The solutions are Eq. (8) and Eq. (15) given above, solutions made possible by the fact that η_2 becomes constant at $\eta_0 = \eta^*$.

To obtain the Boussinesq limit of Eq. (18) set $A = 0$ in $F_{1,2}$:

$$F_1 \to F_1^B \equiv -c^2 k^2 / 8(1+c), \tag{20a}$$

and

$$F_2 \to F_2^B \equiv -k[(1+2c)\eta_2 + ck/4]/(1+c). \tag{20b}$$

One can calculate numerically the solutions η and η^B from the above equations and form R^B. If $\eta_0 = \eta^*$ the results are identical to Figs. (2) and (3), but differ (though not by much) at other values of η_0. This is true unless η_0 is extremely large in which case Eq. (18), with the original F_1 and F_2, fails completely, as we have pointed out previously[28]. The value where this happens is given by

$$(\eta_0 k)_{\max} \equiv \frac{c}{2(1+c)}\left[1+\sqrt{1+\frac{4(1+c)}{Ac^2}}\right]. \tag{21}$$

This expression is derived[27,28] by setting $F_1 = 0$ and this is the reason Eq. (18) fails, giving an unphysical $\eta(t)$ that decreases (!) with time.

Now, F_1^B does *not* have such a zero – from Eq. (20a), it is always negative. It follows that Goncharov's model in the B.A. does not suffer from this large-η_0 breakdown and indeed, from Eq. (21), $(\eta_0)_{\max} \to \infty$ as $A \to 0$, meaning any value of η_0 is admissible in that limit.

We compare the different models in Fig. 4 where we show the results of running a CALE simulation with the same input as Fig. 1(b) but with a 6 times larger $\eta_0 = 2(\eta_0)_{\max} = 0.78$ cm. The CALE results for the bubble amplitude are compared with Eq. (8) and its Boussinesq equivalent Eq. (12), and also with Eq. (18) which gives the negative η, while its Boussinesq equivalent, using F_1^B and F_2^B, circumvents that problem. Needless to say, the Boussinesq limit of Goncharov's equations is a much better description of η^{bubble} at large η_0.

IV. TURBULENT STAGE

A number of experiments[29-33] have shown that rather simple laws govern RT turbulent mixing widths:

$$h^{bubble,spike} = \alpha^{bubble,spike} gAt^2 \tag{22}$$

where $\alpha^{bubble,spike}$ are "constants" depending only on A. Clearly, this is where "extra" A terms might appear. As always, for low A $\alpha^{spike} \approx \alpha^{bubble}$, but at high A α^{spike} is much larger than α^{bubble}, reaching $\sim 4.5\alpha^{bubble}$ near $A \approx 1$. It follows that the B.A. is not a good approximation for h^{spike} except in the traditional low-A region. On the other hand, α^{bubble} is observed[29-33] to be independent of A and is in the range 0.05-0.07. It follows that the B.A. is an excellent approximation for h^{bubble} because A appears only in the combination gA, the same as in the linear regime (Eq. (6a)).

As for RM mixing, we had proposed[34]

$$h^{bubble,spike} = 2\alpha^{bubble,spike} \Delta v A t, \tag{23}$$

an expression that is consistent with recent experiments[35-38]. It follows that, just like the RT case, the B.A. is not a good one for the spike but is excellent for the bubble. This is important because it implies that treatments using the B.A. may apply to bubbles at all Atwood numbers in both RT and RM turbulence.

V. CONCLUSIONS

We saw in Sec. I that scaling arguments, based on the available dimensionless variables in RT and RM problems, can go far in determining the behavior of the Boussinesq ratio R^B. By setting $A = 0$ in the B.A. (except in gA or $\Delta v A$) one takes bubble~spike since there is no more a distinction between high density and low density fluids. This is a poor approximation at high A

since the spikes get substantially longer than bubbles as is well-known and is illustrated in Fig. 1. Bubbles, by contrast, are much less sensitive to A and the B.A. is acceptable even at the extreme limit $A=1$. As far as we know there is no general argument as to whether the B.A. underestimates or overestimates the true value. Using a Layzer-type model we found that $1 \le R^B \le \sqrt{1+A}$ for the RT case, so it overestimates η^{bubble} but the error is at most ~41%, as shown in Fig. 2. For RM we find that the B.A. again overestimates η^{bubble} and R^B can be larger at very late times but at relatively early times it also falls within the 41% estimate (Fig. 3).

One may call the B.A. a "broken symmetry" because it is "almost" valid. It is a perfectly good symmetry in the two extreme, linear and turbulent, regimes as far as the bubble is concerned, but broken in the intermediate, nonlinear regime. Note, however, that the symmetry breaking is not large.

Another way to use the B.A. or to assess its validity is to note that under the B.A. two problems with different A's but the *same* g would be related by a simple $1/\sqrt{A}$ scaling in time. In Fig. 5 we compare Fig.1(a) ($A=0.05$, $t=20$ ms) with another problem having the same g but 9 times larger $A=0.45$, now at $t=20/\sqrt{9}=20/3\approx 6.67$ ms . Comparing bubbles we get 1.56 cm (low A) vs. 1.46 cm (high A). Such a simple $t\sim 1/\sqrt{A}$ scaling would not hold in the full η^{bubble} where A appears in many places. Of course for RM the scaling is $t\sim 1/A$.

Perhaps the most important conclusion of this work is that earlier considerations of the B.A. in RT instabilities[15-18] can be extended to larger A. Similarly, future applications of the B.A. in RM instabilities need not be restricted to low A as far as the bubble is concerned. Indeed, the fully turbulent bubble mixing widths show no distinction between low A and high

A beyond its Boussinesq appearance in gA or $\Delta v A$, as evidenced by α^{bubble} being independent of A; Non-Boussinesq effects appear only in the highly A–dependent α^{spike}.

Acknowledgement

This work was performed under the auspices of the U.S. Department of Energy by Lawrence Livermore National Laboratory under Contract DE-AC52-07NA27344.

APPENDIX: $C_1 < 0$

Start with the RT case, Eq. (13), and show that $F(x)$, defined by

$$F(x) \equiv (3-c)x\tanh x - 4\ln(\cosh x), \tag{A1}$$

satisfies the following 3 properties:

$$\text{i) } F(x) < 0, \quad x \approx 0,$$

$$\text{ii) } F(x) < 0, \quad x \to \infty,$$

$$\text{iii) } \frac{dF}{dx} \neq 0, \quad 0 < x < \infty. \tag{A2}$$

Expanding $F(x)$ near $x \approx 0$ we find $F(x) = -(c-1)x^2 - (2-c)x^4/3$ which is negative for both $c = 1$ or $c = 2$. As $x \to \infty$, $F \to -(c+1)x$ which is also negative. Finally, assume $dF/dx = 0$; this implies

$$\sinh(2x) = \frac{2(3-c)}{1+c}x. \tag{A3}$$

For (A3) to be correct the slope of the left-hand-side near $x = 0$ must be *less* than the slope of the right-hand-side, that is

$$2 < \frac{2(3-c)}{1+c} \tag{A4}$$

which implies $c < 1$, contradicting the definition that $c = 1$ or $c = 2$. It follows that $dF/dx \neq 0$ which completes the proof that $F(x) < 0$ for all $0 < x < \infty$.

The steps are the same for the RM case where, from Eq. (17),

$$F(x) \equiv \frac{x}{1+x} - \ln(1+x)\,. \tag{A5}$$

i) $F(x \approx 0) = -x^2/2 < 0$; ii) $F(x \to \infty) = 1 - \ln(1+x) < 0$; and iii) $dF/dx = -x/(1+x)^2$ never vanishes for $0 < x < \infty$. It follows that $F(x) < 0$ for all $0 < x < \infty$.

REFERENCES

[1]Lord Rayleigh, *Scientific Papers*, **2**, (Dover, New York, 1965).

[2] G. I. Taylor, "The instability of liquid surfaces when accelerated in a direction perpendicular to their planes, I," Proc. R. Soc. London, Ser. A **201**, 192 (1950).

[3]R. D. Richtmyer, "Taylor instability in shock acceleration of compressible fluids," Commun. Pure Appl. Math. **13**, 297 (1960).

[4] E. E. Meshkov, "Instability of the interface of two gases accelerated by a shock wave," Fluid Dyn. **4**, 101 (1969).

[5]D. H. Sharp, "An overview of Rayleigh-Taylor instability," Physica D **12**, 3 (1984).

[6]H. J. Kull, "Theory of the Rayleigh-Taylor instability," Phys. Rep. **206**, 197 (1991).

[7]M. Brouillette, "The Richtmyer-Meshkov instability," Annu. Rev. Fluid Mech. **34**, 445 (2002).

[8]J. D. Lindl, *Inertial Confinement Fusion* (Springer, New York, 1998).

[9]J. Nuckolls, L. Wood, A. Thiessen, and G. Zimmerman, "Laser Compression of Matter to Super-High Densities: Thermonuclear (CTR) Applications," Nature **239**, 139 (1972).

[10]S. P. Regan, R. Epstein, B. A. Hammel, L. J. Suter, H. A. Scott, M. A. Barrios, D. K. Bradley, D. A. Callahan, C. Cerjan, G. W. Collins, S. N. Dixit, T. Doppner, M. J. Edwards, D. R. Farley, K. B. Fournier, S. Glenn, S. H. Glenzer, I. E. Golovkin, S. W. Haan, A. Hamza, D. G. Hicks, N. Izumi, O. S. Jones, J. D. Kilkenny, J. L. Kline, G. A. Kyrala, O. L. Landen, T. Ma, J. J. MacFarlane, A. J. MacKinnon, R. C. Mancini, R. L. McCrory, N. B. Meezan, D. D. Meyerhofer, A. Nikroo, H.- S. Park, J. Ralph, B. A. Remington, T. C. Sangster, V. A. Smalyuk, P. T. Springer, and R. P. J. Town, "Hot-Spot Mix in Ignition-Scale Inertial Confinement Fusion Targets," Phys. Rev. Lett. **111**, 045001 (2013).

[11]W. H. Liu, L.F. Wang, W. H. Ye, and X. T. He, "Nonlinear saturation amplitudes in classical Rayleigh-Taylor instability at arbitrary Atwood number," Phys. Plas. **19**, 042705 (2012).

[12]K. O. Mikaelian, "Growth rate of the Richtmyer-Meshkov instability at shocked interfaces," Phys. Rev. Lett. **71**, 2903 (1993); "Freeze-out and the effect of compressibility in the Ricthmyer-Meshkov instability," Phys. Fluids **6**, 356 (1994).

[13]J. Boussinesq, *Théorie de l'écoulement tourbillonnant et tumultueux des liquides dans les lits rectilignes a grande section*, **1** (Gauthier-Villars et fils, Paris, 1897).

[14]S. Chandrasekhar, *Hydrodynamic and hydromagnetic stability*, (Oxford University Press, London, 1968).

[15]H. Aref and G. Tryggvason, "Model of Rayleigh-Taylor instability," Phys. Rev. Lett. **62**, 749 (1989).

[16]A. Pumir and E. D. Siggia, "Development of singular solutions to the axisymmetrical Euler equations," Phys. Fluids A **4**, 1472 (1992).

[17]M. Chertkov, “Phenomenology of Rayleigh-Taylor turbulence,” Phys. Rev. Lett. **91**, 115001 (2003).

[18]J. R. Ristorcelli and T. T. Clark, “Rayleigh-Taylor turbulence: Self-similar analysis and direct numerical simulations,” J. Fluid Mech. **507**, 213 (2004).

[19]K. O. Mikaelian, “Explicit expressions for the evolution of single-mode Rayleigh-Taylor and Richtmyer-Meshkov instabilities at arbitrary Atwood numbers,” Phys. Rev. E **67**, 026319 (2003).

[20]D. J. Lewis, “The instability of liquid surfaces when accelerated in a direction perpendicular to their planes.II,” Proc. R. Soc. London, Ser. A **202**, 81 (1950).

[21]R. E. Tipton, in *Megagauss Technology and Pulsed Power Applications*, edited by C. M. Fowler, R. S. Caird, and D. J. Erickson (Plenum, New York, 1987); R. T. Barton, in *Numerical Astrophysics*, edited by J. M. Centrella, J. M. LeBlanc, R. L. Bowers, and J. A. Wheeler (Jones and Bartlett, Boston, 1985).

[22]D. Layzer, “On the instability of superposed fluids in a gravitational field,” Astrophys. J. **122**, 1 (1955).

[23]J. Hecht, U. Alon, and D. Shvarts, “Potential flow models of Rayleigh-Taylor and Richtmyer-Meshkov bubble fronts,” Phys. Fluids **6**, 4019 (1994).

[24]K. O. Mikaelian, “Analytic approach to nonlinear Rayleigh-Taylor and Richtmyer-Meshkov instabilities,” Phys. Rev. Lett. **80**, 508 (1998).

[25]Q. Zhang, “Analytical solutions of Layzer-type approach to unstable interfacial fluid mixing,” Phys. Rev. Lett. **81**, 3391 (1998).

[26]V. N. Goncharov, “Analytical model of nonlinear, single-mode, classical Rayleigh-Taylor instability at arbitrary Atwood numbers,” Phys. Rev. Lett. **88**, 134502 (2002).

[27]K. O. Mikaelian, “Reshocks, rarefactions, and the generalized Layzer model for hydrodynamic instabilities,” Phys. Fluids **21**, 024103 (2009).

[28]K. O. Mikaelian, “Limitations and failures of the Layzer model for hydrodynamic instabilities,” Phys. Rev. E **78**, 015303 (2008).

[29]K. I. Read, “Experimental investigation of turbulent mixing by Rayleigh-Taylor instability,” Physica D **12**, 45 (1984).

[30]D. M. Snider and M. J. Andrews, “Rayleigh-Taylor and shear driven mixing with an unstable thermal stratification,” Phys. Fluids **6**, 3324 (1994).

[31]M. B. Schneider, G. Dimonte, and B. Remington, “Large and small scale structure in Rayleigh-Taylor mixing,” Phys. Rev. Lett. 80, 3507 (1998).

[32]G. Dimonte and M. Schneider, “Density ratio dependence of Rayleigh-Taylor mixing for sustained and impulsive acceleration histories,” Phys. Fluids **12**, 304 (2000).

[33]P. Ramaprabhu and M. J. Andrews, “Experimental investigation of Rayleigh-Taylor mixing at small atwood numbers,” J. Fluid Mech. **502**, 233 (2004).

[34]K. O. Mikaelian, “Turbulent mixing generated by Rayleigh-Taylor and Richtmyer-Meshkov instabilities,” Physica D **36**, 343 (1989).

[35]M. Vetter and B. Sturtevant, “Experiments on the Richtmyer-Meshkov instability of an air/SF_6 interface,” Shock Waves **4**, 247 (1995).

[36]HH. Shi, G. Zhang, K. Du, and HX. Jia, “Experimental study on the mechanism of the Richtmyer-Meshkov instability at a gas-liquid interface,” J. Hydrodynamics **21**, 423 (2009).

[37]E. Leinov, G. Malamud, Y. Elbaz, L. A. Levin, G. Ben-Dor, D. Shvarts, and O. Sadot, "Experimental and numerical investigation of the Richtmyer-Meshkov instability under re-shock conditions," J. Fluid Mech. **626**, 449 (2009).

[38]J. W. Jacobs, V. V. krivets, V. Tsiklashvili, and O. A. Likhachev, "Experiments on the Richtmyer-Meshkov instability with an imposed, random initial perturbation," Shock Waves **23**, 407 (2013).

Figure Captions:

Fig. 1. Two RT and two RM simulations comparing low-A and high-A problems keeping gA (for RT) and $\Delta v A$ (for RM) the same. The parameters defining (a) are $g = 0.66\,\text{cm/ms}^2$, $A = 0.05$, $\lambda = 2.43\,\text{cm}$, and $\eta_0 = 0.13\,\text{cm}$. For (b) we let $g \to g/19$, $A \to 19A = 0.95$, keeping the same λ and η_0. (c) is defined by $\Delta v = 41\,\text{cm/ms}$, $A = 0.1$, $\lambda = 2.0\,\text{cm}$, and $\eta_0 = 0.1\,\text{cm}$. For (d) we let $\Delta v \to \Delta v/7.5$, $A \to 7.5A = 0.75$, keeping the same λ and η_0. The arrows indicate the location of an unperturbed interface relative to which bubbles (below the arrows) and spikes (above the arrows) are defined. The main difference between low-A and high-A lies in the spike behavior; bubbles are much less sensitive and amenable to the Boussinesq approximation.

Fig. 2. The Boussinesq ratio R^B calculated from Eqs. (8) and (12) for bubbles generated by the RT instability. Black lines refer to 2D, i.e., $c = 2$, and red refers to 3D or $c = 1$. The initial $\eta_0 k$ is set equal to $1/(1+c)$. Note that $R^B_{2D} > R^B_{3D}$.

Fig. 3. Same as Fig. 3 for the RM case calculated using Eqs. (15) and (16). Note that $R^B_{2D} < R^B_{3D}$.

Fig. 4. Bubble amplitude versus time for a problem just like the one shown in Fig. 1b but with a six times larger initial amplitude: $\eta_0 = 2(\eta_0)_{\max} = 0.78$ cm, where $(\eta_0)_{\max}$ is defined by Eq. (21). Eq. (18) fails for any $\eta_0 \geq (\eta_0)_{\max}$. Its Boussinesq version, obtained by setting $A = 0$ except in the gA term, gives reasonable results. Eqs. (8) and its Boussinesq version, Eq. (12), come closer to the CALE calculation.

Fig. 5. Comparison of (a) low-A, late time simulation with (b) high-A, early time simulation, keeping everything else the same. Fig. 5(a) is the same as Fig. 1(a); in Fig.5(b) A has been increased 9-fold and the snapshot taken 3 times earlier, confirming $\sqrt{A}t$ Boussinesq scaling.

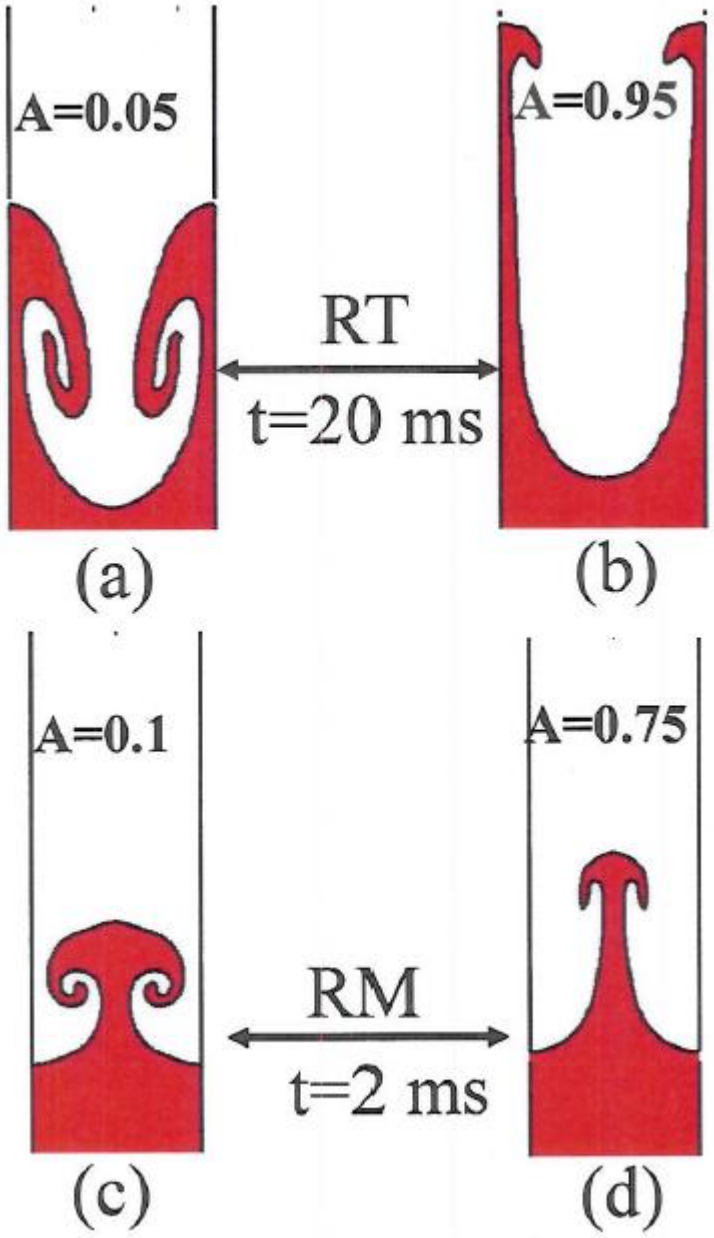

Fig. 1

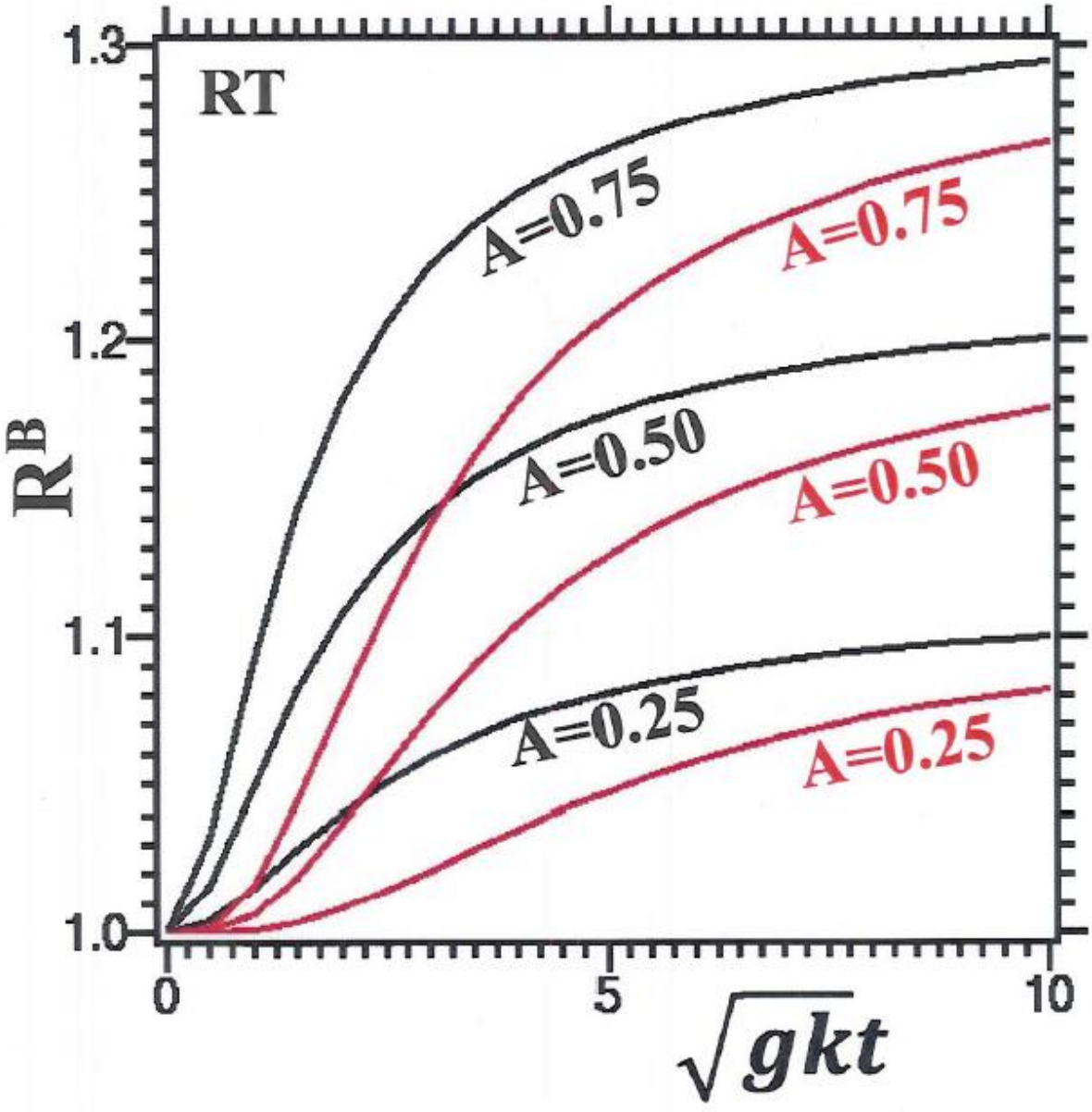

Fig. 2

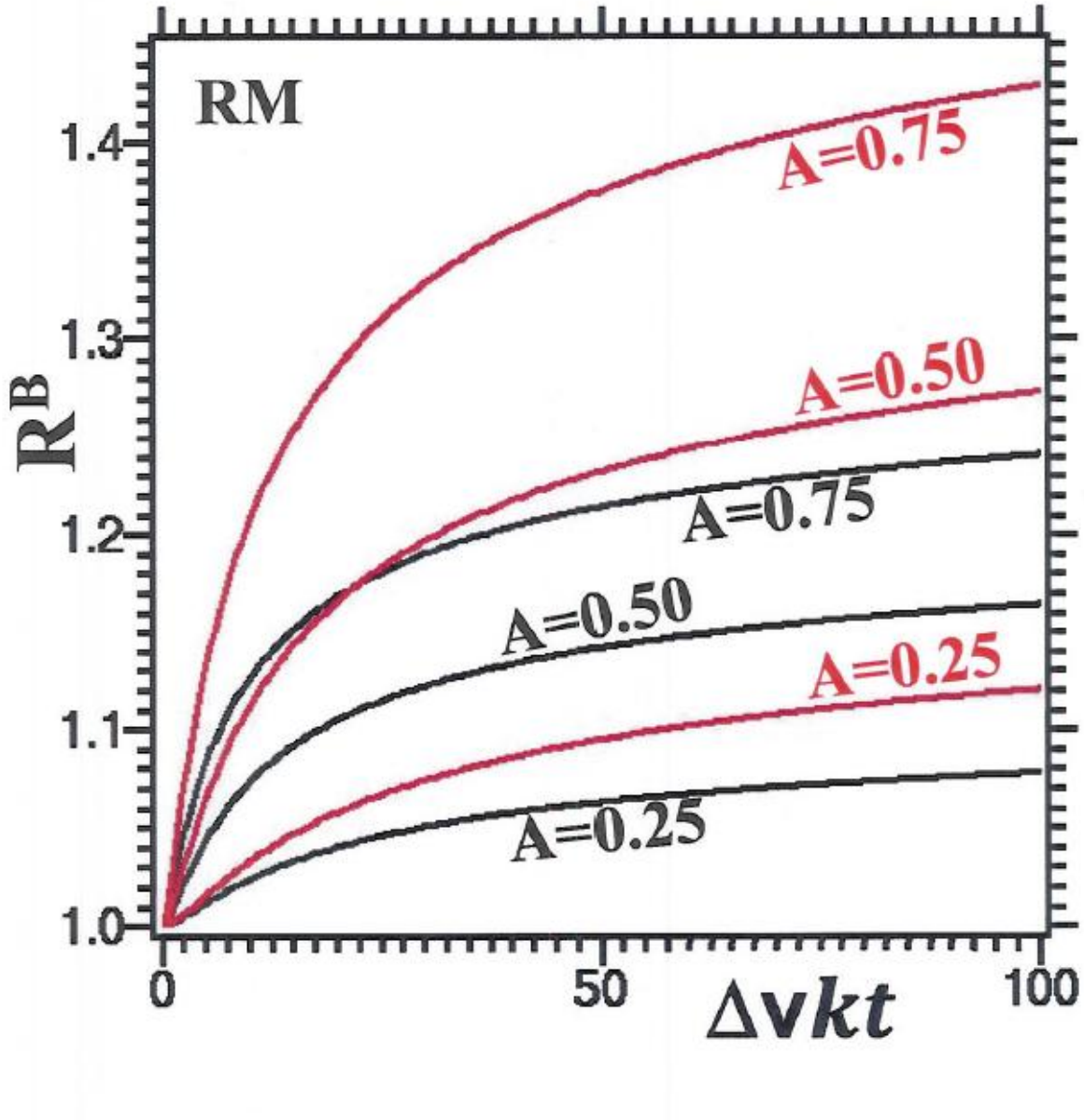

Fig.3

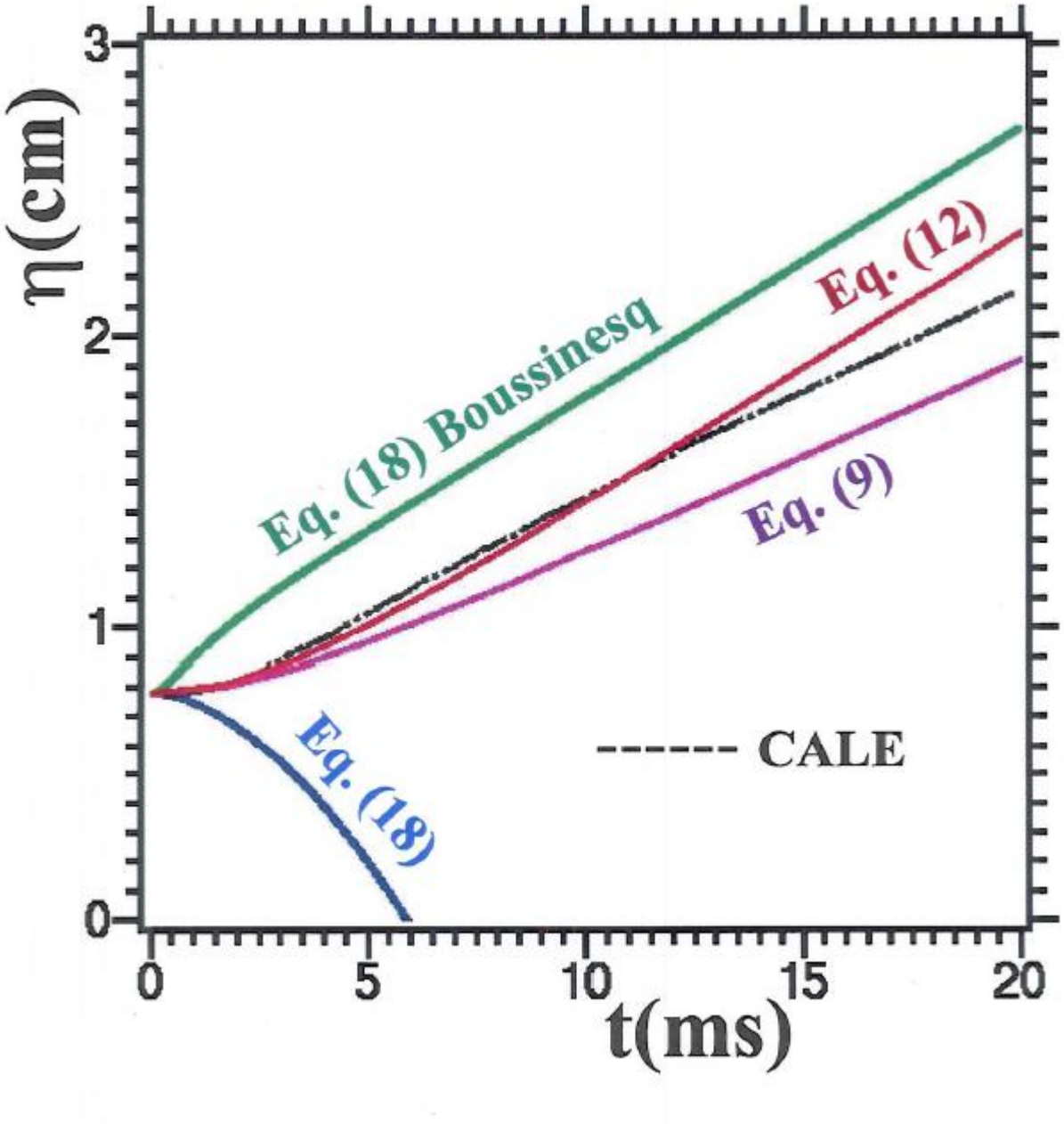

Fig. 4

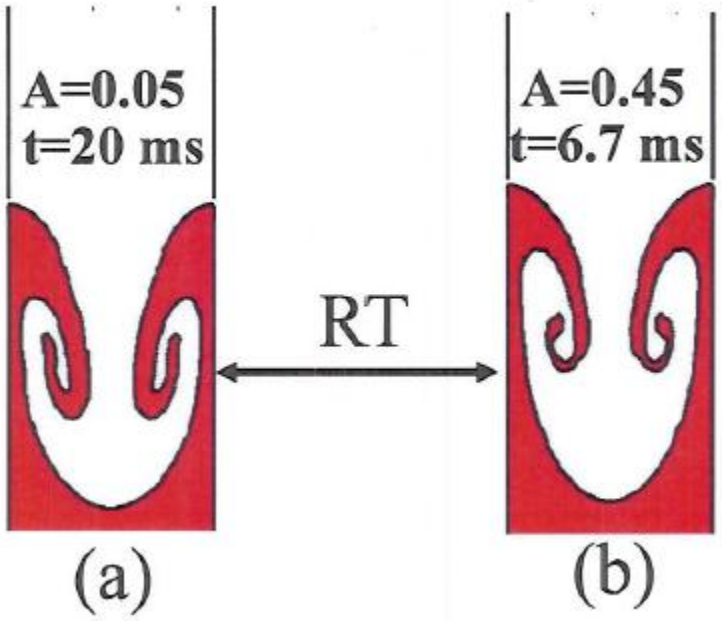

Fig. 5